Dalton Transactions

PAPER

View Article Online
View Journal | View Issue

Check for updates

Cite this: *Dalton Trans.*, 2019, **48**, 16258

C–H and C–F bond activation reactions of pentafluorostyrene at rhodium complexes†‡

Conghui Xu, Maria Talavera, Stefan Sander and Thomas Braun *

Received 18th August 2019,
Accepted 9th October 2019

DOI: 10.1039/c9dt03371h

rsc.li/dalton

The rhodium(I) complexes [Rh(Bpin)(PEt$_3$)$_3$] (**1**), [Rh(H)(PEt$_3$)$_3$] (**5**) and [Rh(Me)(PEt$_3$)$_3$] (**14**) were employed in reactions with pentafluorostyrene affording coordination of the olefin and C–F or C–H bond activation. Control of the reaction conditions allowed for selective activation reactions at different positions at the fluorinated aromatic ring. The rhodacycle *trans*-[Rh(F)(CH$_2$CH$_2$(2-C$_6$F$_4$))(PEt$_3$)$_2$] (**7**) was identified as an intermediate for an activation at the 2-position. Reactivity studies of the latter with CO led to the generation of *trans*-[Rh(F)(CH$_2$CH$_2$C$_6$F$_4$)(CO)(PEt$_3$)$_2$] (**10**). Stoichiometric and catalytic hydroboration reactions were achieved using complexes **1** or **5** as catalysts.

Published on 16 Nhlangula 2019. Downloaded by Fail Open on 2025-05-07 08:30:15.

Introduction

Introducing fluorine atoms to organic compounds not only changes their chemical and biological properties but also provides interesting building blocks for pharmaceuticals, agrochemicals or in material science.[1–3] In the last two decades it was demonstrated that fluorinated olefins and aromatic compounds can undergo C–H or C–F bond activation reactions at rhodium complexes, which opens up unique opportunities for functionalization.[4–16]

Perfluorinated styrene is an important starting material for a lot of catalytic reactions, such as C–C coupling,[17] epoxidation,[18] hydrogenation,[19,20] hydroformylation[21] and hydroboration.[22–29] In the past, the hydroboration of pentafluorostyrene mediated by rhodium complexes was achieved with high selectivity.[23–27] In these reactions, the borane source can be critical and Ramachandran *et al.*,[23,27] Brown *et al.*[25] and Segarra *et al.*[24] showed that HBcat (catechol borane) can afford Markovnikov hydroboration products using [Rh(COD)(dppb)]BF$_4$, [Rh(Quinap)]OTf or [Rh(COD)(Binap)$_2$]BF$_4$ as catalysts, respectively (dppb = 1,4-bis(diphenylphosphino)butane; Quinap = 1-(2-diphenylphosphino-1-naphthyl)isoquinoline; Binap = 2,2′-bis(diphenylphosphino)-1,1′-binaphthyl). However, Westcott and co-workers[26] disclosed that HBpin (pinacol borane) yields Markovnikov addition products in a low selectivity when employing [Rh(acac)(κ^2-*o*-Ph$_2$PC$_6$H$_4$CH=N-2,6-iPr$_2$C$_6$H$_3$)] as a catalyst. In 1993, Herrmann *et al.* reported a stoichiometric reaction using pentafluorostyrene and osmium tetroxide to form a fluorinated osmate ester quantitatively by a cycloaddition reaction.[30] In addition, Perutz and coworkers described the coordination of pentafluorostyrene at nickel.[31] However, to the best of our knowledge, stoichiometric activation reactions of pentafluorostyrene derivatives with rhodium complexes, which might be crucial for an understanding of the conversions named above, are still unknown.

Herein we describe the stoichiometric reactivities of [Rh(Bpin)(PEt$_3$)$_3$] (**1**), [Rh(H)(PEt$_3$)$_3$] (**5**) and [Rh(Me)(PEt$_3$)$_3$] (**14**) towards pentafluorostyrene. Reaction pathways are versatile providing coordination, C–F bond activation or C–H bond activation products. In addition, the hydroboration of pentafluorostyrene with HBpin and [Rh(Bpin)(PEt$_3$)$_3$] (**1**) or [Rh(H)(PEt$_3$)$_3$] (**5**) as a catalyst was studied to obtain fluorinated building blocks by regioselective Markovnikov addition.

Results and discussion

Coordination of fluorinated styrene derivatives

Treatment of the rhodium boryl complex [Rh(Bpin)(PEt$_3$)$_3$] (**1**)[32,33] with an excess amount of pentafluorostyrene (ratio 1 : 1.2) in d_{14}-methylcyclohexane at room temperature for 5 min afforded the two complexes *fac*-[Rh(H)(η^2-CH$_2$CHC$_6$F$_5$)(PEt$_3$)$_3$] (**2**) and *fac*-[Rh(H)(η^2-CH(Bpin)CHC$_6$F$_5$)(PEt$_3$)$_3$] (**3**) as well as the borylated olefin *E*-BpinCH=CHC$_6$F$_5$ (**4**) in a ratio of 1.8 : 1 : 0.6 (based on the ^{19}F NMR spectrum) (Scheme 1). In contrast, when treating complex **1** with pentafluorostyrene in a ratio of 2.5 : 1, complex **3** was generated together with the rhodium hydrido complex [Rh(H)(PEt$_3$)$_3$] (**5**)[34] (Scheme 1).

Humboldt-Universität zu Berlin, Department of Chemistry, Brook-Taylor-Straße 2, 12489 Berlin, Germany. E-mail: thomas.braun@cms.hu-berlin.de; Tel: +49 30 2093 3913

† Dedicated to Prof. Robin Perutz on the occasion of his 70th birthday.

‡ Electronic supplementary information (ESI) available: Synthesis and analytics for all compounds, *xyz* coordinates for the DFT calculation optimized structure and X-ray data. CCDC 1956127. For ESI and crystallographic data in CIF or other electronic format see DOI: 10.1039/c9dt03371h

This journal is © The Royal Society of Chemistry 2019

Published on 16 Nhlangula 2019. Downloaded by Fail Open on 2025-05-07 08:30:15.

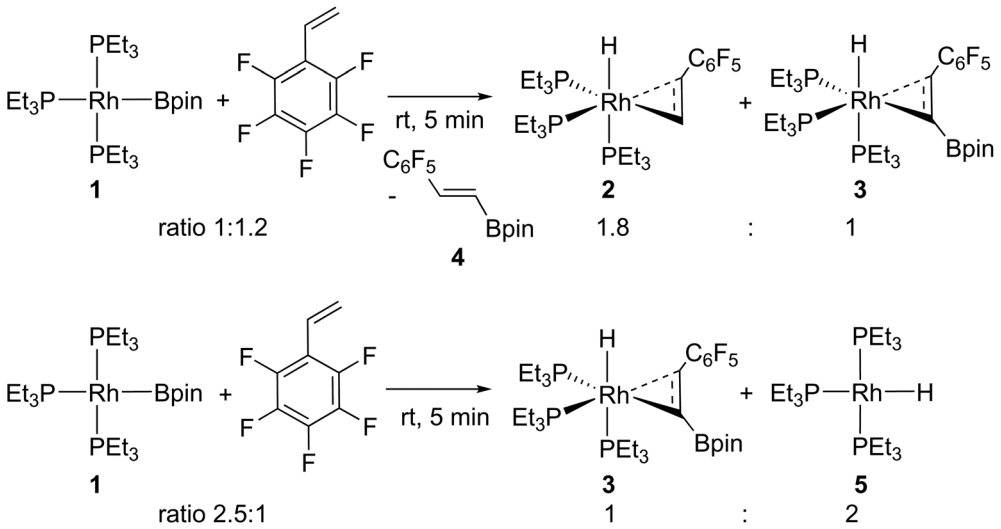

Scheme 1 Stoichiometric reactions of complex **1** with pentafluorostyrene.

Note that the complexes **2** and **3** (for their characterization see below) are in solution only stable at low temperature for long periods of time and converted further by C–F bond activation (see below). Therefore, after their preparation at room temperature within 5 minutes, the characterization was performed at 213 K as recently reported for other similar rhodium complexes such as *fac*-[Rh(H)(η^2-CH_2CHCF_3)(PEt_3)$_3$][6] and *fac*-[Rh(H)(η^2-CH_2CFCF_3)(PEt_3)$_3$].[35]

In the ^{1}H NMR spectrum of compound **4** (for the independent synthesis see ESI‡) two doublet signals appeared at 7.48 and 6.70 ppm which are assigned to the olefinic moiety. The coupling constant of 18.8 Hz is indicative of a *trans* arrangement.[36] In the ^{19}F NMR spectrum three signals appeared as multiplets at −144.0, −155.5 and −163.5 ppm, respectively, in a ratio of 2 : 1 : 2. A peak in the GC-MS of *m*/*z* 320 supports the proposed structure.

Three broad resonances for **2** were observed in the ^{31}P{^{1}H} NMR spectrum indicating a dynamic process, which is presumably associated with a rotation about the olefinic double bond. The ^{31}P{^{1}H} NMR spectrum at 213 K revealed three signals at 20.3, 13.7 and 5.8 ppm in a ratio of 1 : 1 : 1, which is consistent with the *fac*-configuration.[6] The doublet of doublet of doublets ($^1J_{(P,Rh)}$ = 139.8, $^2J_{(P,P)}$ = 42.6, $^2J_{(P,P)}$ = 24.2 Hz) at 20.3 ppm and a doublet of doublet of doublets ($^1J_{(P,Rh)}$ = 134.0, $^2J_{(P,P)}$ = 42.9, $^2J_{(P,P)}$ = 28.8 Hz) at 13.7 ppm were assigned to the phosphine ligands in the *trans* position to the CHC_6F_5 and CH_2 moieties. The doublet of multiplets at 5.8 ppm with a coupling of 95.8 Hz to the rhodium atom belongs to the phosphine ligand in *trans* position to the hydrido ligand. The large *trans* influence of the hydrido ligand is in accordance with the smaller coupling constant.[6,37,38] The values of the rhodium–phosphorus coupling constants suggest the presence of a Rh(I) complex.[5,6,32,39] In the ^{1}H NMR spectrum of **2** at 213 K three broad signals appeared at 3.32, 3.05 and 1.83 ppm for the olefinic protons, which is consistent with data for the previously reported complex *fac*-[Rh(H)(η^2-CH_2CHCF_3)(PEt_3)$_3$].[6] In the ^{1}H NMR spectrum, for the rhodium-bound hydrido ligand, a doublet of triplet of doublets with a coupling of 161.8 Hz to the *trans* phosphine ligand, 19.8 Hz to the *cis* phosphine ligands and 9.2 Hz to the rhodium atom appeared at −14.64 ppm. The ^{19}F NMR spectrum at room temperature also reflects the dynamic process with three broad signals in a ratio of 2 : 2 : 1. In the ^{19}F NMR spectrum at 213 K, five resonances appeared in a ratio of 1 : 1 : 1 : 1 : 1. Signals at −146.0 and −146.7 ppm are presumably due to the two fluorine atoms in the *ortho* position, while signals at −166.3 and −167.0 ppm belong to the two *meta* fluorine atoms and the signal at −170.9 ppm can be assigned to the *para* fluorine atom.[40–43]

The ^{31}P{^{1}H} NMR spectrum of **3** at 213 K showed three signals comparable to the ones for complex **2** at 18.2, 15.3 and 3.3 ppm. However, only two signals appeared at 3.97 and 3.10 ppm in the ^{1}H NMR spectrum with a proton–proton coupling constant of 12.0 Hz in the ^{1}H{^{31}P} NMR spectrum for the protons of the coordinated olefin moiety. The absence of one proton suggests its substitution by the Bpin group. The hydrido ligand appeared as a doublet of triplet of doublets at −14.87 ppm. The resonance has a coupling constant of 163.0 Hz to the *trans* phosphorus atom, 18.2 Hz to the two *cis* phosphorus atoms and 5.5 Hz to the rhodium atom. In the ^{19}F NMR spectrum, five signals, similar to the ones of complex **2**, appeared at −144.2, −145.0, −166.5, −167.1 and −170.4 ppm. DFT calculations of **3** were performed (BP86/def2-SVP). The structural optimization of the possible rotational isomers of complex **3** showed that the isomer with the lower energy (favored by 21.2 kJ mol^{-1}) has the Bpin group and hydrido ligand orientated on the same side of a plane defined by the rhodium center and the olefin, while the fluorinated moiety remains positioned on the other side.

A conceivable mechanistic pathway for the observed reactivity is depicted in Scheme 2. After coordination of pentafluorostyrene at complex **1** the insertion of the olefin into the Rh–B bond occurs. A β-hydride elimination would then lead to

Published on 16 Nhlangula 2019. Downloaded by Fail Open on 2025-05-07 08:30:15.

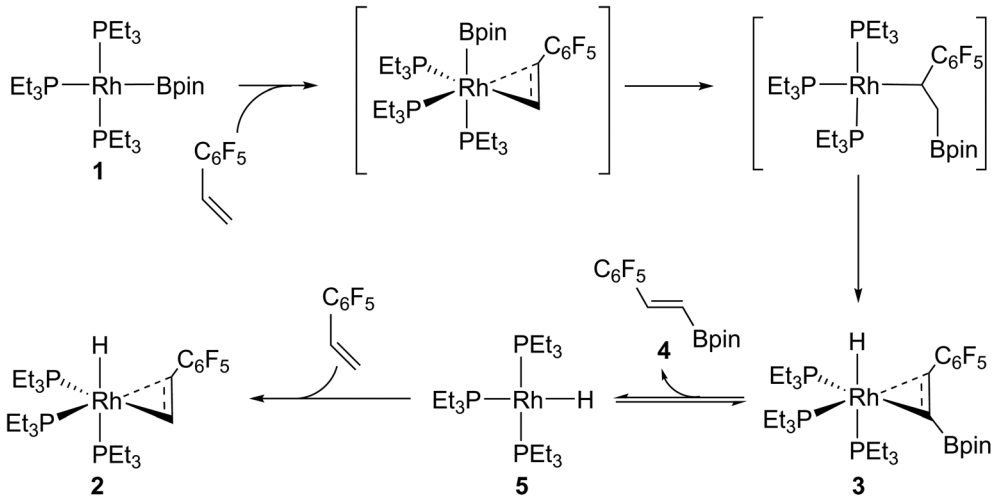

Scheme 2 Possible mechanism for the formation of complexes **2** and **3**.

complex **3** and subsequently **4** and **5** are formed initially and results in **3** after olefin coordination. In the presence of an excess of pentafluorostyrene, its coordination to **5** yields complex **2**. Note that a reaction of complex **1** with stoichiometric amounts of styrene leading to a dehydrogenative borylation at the double bond and complex **5** was reported,[44] but the coordination of the olefinic product was not observed.

C–F bond activation reactions

To confirm the structures of complexes **2** and **3** as well as the proposed mechanism, independent reactions between pentafluorostyrene or the boryl derivative **4** and the rhodium hydrido complex $[Rh(H)(PEt_3)_3]$ (**5**) were performed.

Indeed, treatment of **5** with the boryl derivative **4** (ratio 1.7 : 1) in d_8-toluene at 213 K gave after 5 min *fac*-$[Rh(H)(\eta^2\text{-}CH(Bpin)CHC_6F_5)(PEt_3)_3]$ (**3**). Interestingly, after warming up the reaction solution or performing the reaction directly at room temperature for 30 min (ratio 1 : 1.4), the C–F bond activation at the *ortho* position to the olefin moiety was observed yielding $[Rh(2\text{-}C_6F_4CHCH_2)(PEt_3)_3]$ (**6**) as the main product, together with another unidentified complex in a ratio of 13.5 : 1 (based on the $^{31}P\{^1H\}$ NMR spectrum) (Scheme 3). The likely formation of HF might induce deborylation reactions at the olefinic moiety to give fluoroboronates. It is notable that the C–F bond activation[12,45–54] of the boryl derivative at **5** lead to the cleavage of the C–F bond at the *ortho* position to the vinyl group. Comparable *ortho*-directing effects have been observed before at the $\{Rh(PEt_3)_3\}$ fragment in C–F bond activation reactions of fluorinated pyridines and the C–H bond activation of aromatic SCF_3 compounds.[5,9,32,39,55]

The signals in the $^{31}P\{^1H\}$ NMR spectrum for complex **6** were simulated and are depicted in Fig. 1. The coupling constants shown in the $^{31}P\{^1H\}$ NMR spectrum between the rhodium and phosphorus atoms give evidence of a Rh(I) complex.[5,6,32,39] The ^1H NMR spectrum exhibited three resonances as a doublet of doublets ($^3J_{(H,H)}$ = 18.4, $^3J_{(H,H)}$ = 11.8 Hz), a doublet ($^3J_{(H,H)}$ = 18.1 Hz) and a doublet ($^3J_{(H,H)}$ = 11.5 Hz) at 8.16, 6.38 and 5.40 ppm, respectively, due to the olefin moiety of the complex. Four signals were observed in the ^{19}F NMR spectrum, which was also simulated and is depicted in Fig. 2. The assignment of the fluorinated moiety is

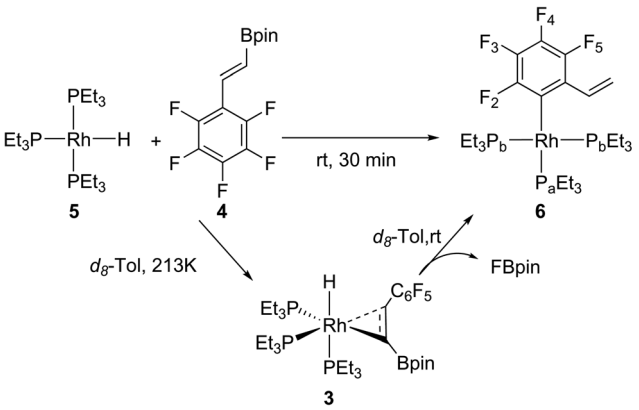

Scheme 3 Independent stoichiometric reaction of complex **5** and compound **4**.

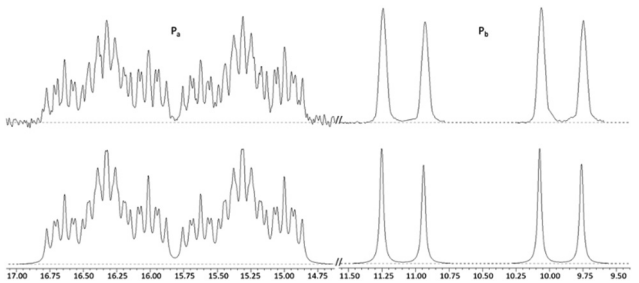

Fig. 1 The $^{31}P\{^1H\}$ NMR spectrum of complex **6**; simulated (below) observed (above) using the following coupling constants (Hz): $^1J_{(Pa,Rh)}$ = 123.3, $^2J_{(Pa,Pb)}$ = 38.0, $^4J_{(Pa,F2)}$ = 14.6, $^5J_{(Pa,F5)}$ = 9.8, $^5J_{(Pa,F3)}$ = 6.6; $^1J_{(Pb,Rh)}$ = 143.3.

 This journal is © The Royal Society of Chemistry 2019

Published on 16 Nhlangula 2019. Downloaded by Fail Open on 2025-05-07 08:30:15.

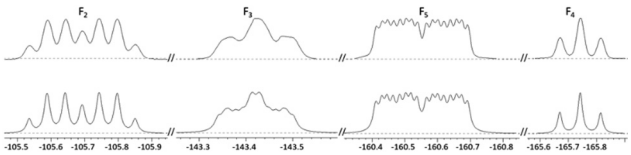

Fig. 2 The ^{19}F NMR spectrum of complex **6**; simulated (below) observed (above) using the following coupling constants (Hz): $^{5}J_{(F2,F5)}$ = 43.8, $^{3}J_{(F2,F3)}$ = 14.6, $^{4}J_{(F2,Pa)}$ = 14.6, $^{3}J_{(F2,Rh)}$ = 14.6, $^{3}J_{(F3,F4)}$ = 20.3, $^{5}J_{(F3,Pa)}$ = 6.6, $^{4}J_{(F3,Rh)}$ = 4.0, $^{3}J_{(F5,F4)}$ = 20.3, $^{5}J_{(F5,Pa)}$ = 9.8, $^{4}J_{(F5,Rh)}$ = 5.2.

based on the comparison with the literature.[39,56–58] The chemical shifts resemble those found for *trans*-[Ni(F)(2,3,4,5-C_6F_4H)-(PEt_3)$_2$].[43] In addition, liquid injection field desorption ionization mass spectrometry (LIFDI MS) revealed a peak at *m*/*z* 632 consistent with the structure of complex **6**.

Similar to the formation of complex **3**, complex **2** can be also independently synthesized by the reaction of [Rh(H)-(PEt_3)$_3$] (**5**) with pentafluorostyrene (ratio 1.4 : 1). Although, complex **2** is more stable, after 1 d at room temperature, it was partially transformed (64% conversion) by cyclometallation and C–F bond activation into the rhodaindane complex *trans*-[Rh(F)(CH_2CH_2(2-C_6F_4))(PEt_3)$_2$] (**7**), free PEt_3, traces of complex *mer*-[Rh(F)(CH_2CH_2(2-C_6F_4))(PEt_3)$_3$] (**8**) and minor amounts of the C–H bond activation complex [Rh(*E*-$CHCHC_6F_5$)(PEt_3)$_3$] (**15**) as well as the hydrogenation product ethylpentafluorobenzene **9** (see below; the low temperature ^{19}F NMR spectrum shows that the ratio of **8** : **9** : **15** is 1 : 0.18 : 0.07)[59] (Scheme 4). Note that the formation of minor amounts of the C–H bond activation product **15** promotes the hydrogenation of pentafluorostyrene to afford compound **9**. Complex **7** and free phosphine are in equilibrium with **8**, and by cooling down a solution at 233 K complex **7** can be converted into complex **8** completely. In fact, after applying vacuum to remove the solvent and some PEt_3, complex **7** cannot be transformed completely into complex **8** at low temperature.

In the ^{31}P{^{1}H} NMR spectrum of **7**, a broad doublet of doublets appeared at 18.4 ppm with a coupling constant of 114.2 Hz to rhodium and 16.6 Hz to the metal-bound fluorido ligand. The ^{1}H NMR spectrum showed two broad signals at 3.20 and 2.45 ppm that belong to the protons of the $C_6F_4CH_2CH_2$ moiety. Two signals appeared at 37.3 ppm and 23.2 ppm as a singlet and doublet with a coupling constant of 32.6 Hz to the rhodium nucleus in the ^{13}C{^{1}H} NMR spectrum. They were assigned to the β and α carbon atoms of complex **7**, respectively. The APT NMR spectrum also confirmed the existence of the two CH_2 moieties. In addition, five signals appeared at −130.6, −141.9, −162.5, −167.3 and −290.6 ppm in the ^{19}F NMR spectrum where the latter resonance corresponds to the rhodium bound fluorido ligand.[60] Geometry optimization performed by DFT calculations (BP86/def2-SVP) revealed a *trans* arrangement of the fluorido ligand and the aromatic ring.

In case of complex **8**, the ^{31}P{^{1}H} NMR spectrum of **8** showed two signals at 7.9 and −2.8 ppm in a 2 : 1 ratio, which appeared as a doublet of doublet of doublets and a doublet of multiplets, respectively. For the phosphine ligands in a mutual *trans* position, the coupling constant of 103.8 Hz to the rhodium atom indicates the presence of a Rh(III) complex,[32,61] while the coupling constants of 29.7, 17.9 Hz are due to couplings to the phosphine and fluorido ligands, respectively. The coupling constant of around 90 Hz for the resonance at −2.8 ppm is due to the coupling to rhodium. Based on a ^{1}H–^{1}H COSY NMR spectrum, two signals at 3.04 and 1.42 ppm in the ^{1}H NMR spectrum were assigned to the CH_2 groups in complex **8**. Comparable to the data for complex **7**, the ^{13}C{^{1}H} NMR spectrum depicted two signals at 37.8 ppm and 23.7 ppm for the β and α carbon atoms. The ^{19}F NMR spectrum displayed five signals, four in the fluoroaromatic region and one at −385.1 ppm characteristic for the rhodium(III) bound fluorido ligand.[10,62,63]

Single crystals suitable for X-ray crystallography of complex **8** were obtained from a concentrated solution in hexane by slow evaporation while letting the solution warm up from 193 K to 278 K (Fig. 3). The structure shows a distorted octahedral geometry of the metal-bound ligands at the rhodium center and the fluorido ligand occupies the *trans* position to the CH_2 group. Note that the location of the fluorido ligand in **7** and **8** is different, because in **7** we suggest the above mentioned *trans* position of the fluorido ligand and the aromatic ring. The Rh1–F1 distance is 2.1360(9) Å, which is slightly longer than in other Rh(III) fluorido complexes.[62,64] Geometry optimization performed by DFT calculations (BP86/def2-SVP) supports the obtained structure for **8** with an energy 12 kJ mol^{-1} lower than the isomer with the fluorido ligand *trans* to the aromatic ring.

Complex **7** can convert slowly into [Rh(2-$C_6F_4CHCH_2$)-(PEt_3)$_3$] (**6**) and presumably HF. The presence of KPF_6 can accelerate the transformation to full conversion within 14 d. The obtaining of complex **6** where the C–F bond activation occurs at the *ortho* position, supports the structural assignment of the rhodacycles.

Mechanistically, for the generation of **7** from complex **2**, an initial insertion of the metal-bound olefin into the rhodium–hydrogen bond is suggested (Scheme 4). Then, an intramolecular oxidative addition of the C–F bond occurs. Note that non-fluorinated metallaindanes have been previously described at Pd and Ni by a C–H orthometallation reaction.[65,66] However, the C–F bond oxidative additions at rhodium are rare and were reported at cyclopentadienyl or tris-pyrazolylborate complexes.[10,67] Complex **6** can subsequently be formed by β-hydride elimination and a subsequent elimination of HF. In the presence of KPF_6 the latter reaction is promoted, because an initial production of KF can endorse a reductive elimination and it can also trap HF by generation of a bifluoride.

To confirm the structural assignment of **7** further, its reactivity towards carbon monoxide was tested, which could occupy a vacant coordination site. Indeed, the 18-electron derivative *trans*-[Rh(F)($CH_2CH_2C_6F_4$)(CO)(PEt_3)$_2$] (**10**) was obtained under CO atmosphere. The isotopologue *trans*-[Rh(F)($CH_2CH_2C_6F_4$)(^{13}CO)(PEt_3)$_2$] (**10′**) was generated after treatment

Published on 16 Nhlangula 2019. Downloaded by Fail Open on 2025-05-07 08:30:15.

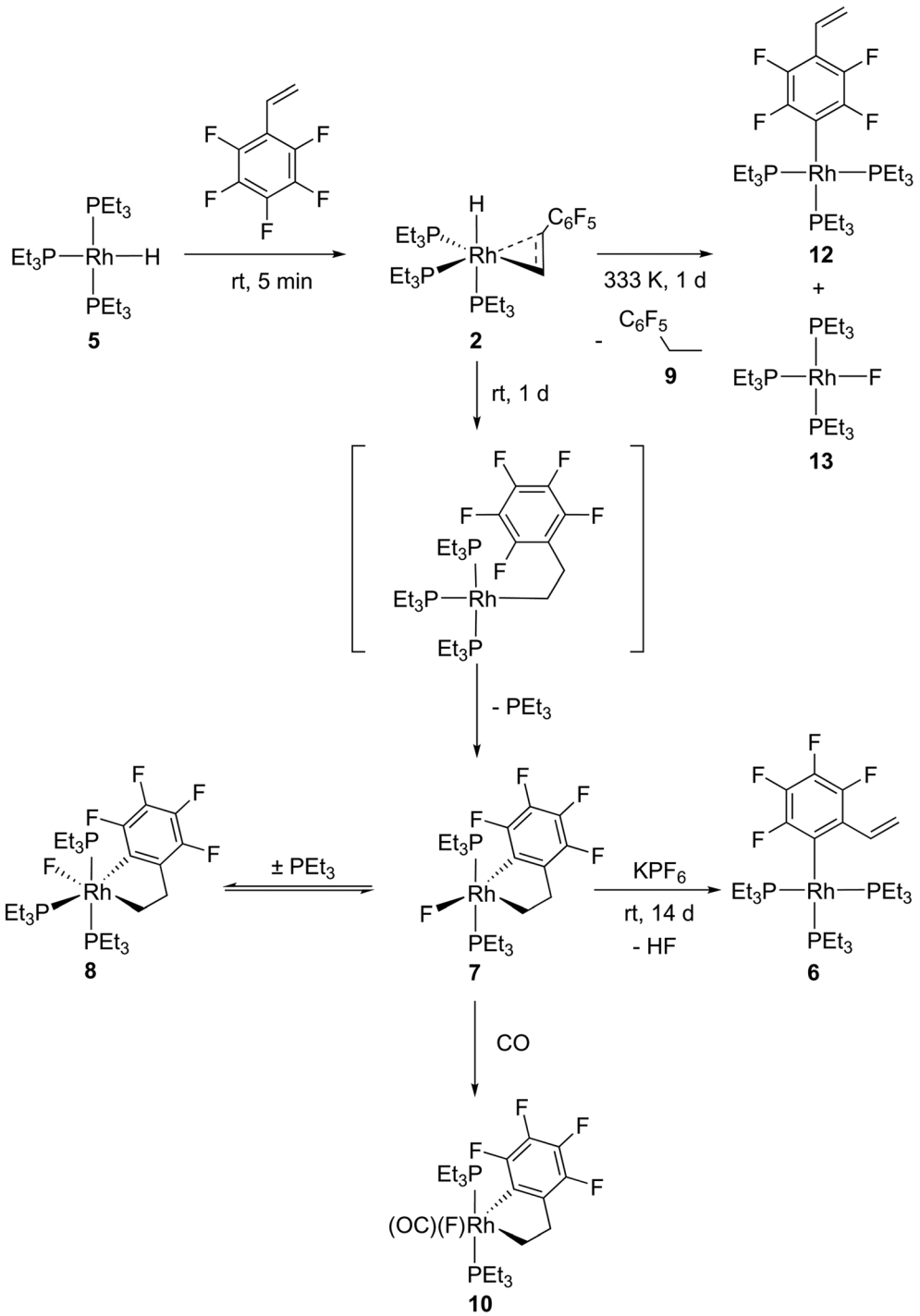

Scheme 4 Stoichiometric reactions of complex **5** with pentafluorostyrene.

of **7** with ^{13}CO. Note that the formation of complex [Rh(H)(CO)-$(PEt_3)_3$] (**11**)[68,69] (or the isotopologue [Rh(H)(^{13}CO)$(PEt_3)_3$] (**11′**), see ESI‡ for characterization) was also observed. Complex **11** stems from the reaction of the remaining complex **2** with CO.

A doublet of doublets at 16.9 ppm with a coupling constant of 98.5 Hz to the rhodium atom and 17.3 Hz to the fluorido ligand can be observed in the $^{31}P\{^1H\}$ NMR spectrum of **10**. For complex **10′** an additional coupling to the labelled carbon atom of 10.9 Hz was detected. The coupling constant is in accordance with a *cis*-configuration of phosphine and CO ligands.[36,44] The ^1H NMR spectrum shows a broad triplet (J = 7.5 Hz) at 3.15 ppm that corresponds to the β carbon at 33.4 ppm in the ^{13}C domain of a ^1H–^{13}C HMQC NMR spectrum. A multiplet at 2.56 ppm in the ^1H domain correlates

 This journal is © The Royal Society of Chemistry 2019

Published on 16 Nhlangula 2019. Downloaded by Fail Open on 2025-05-07 08:30:15.

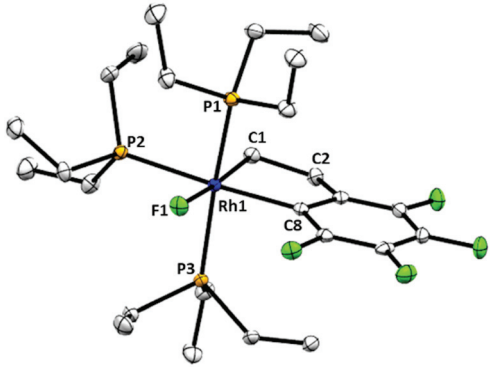

Fig. 3 ORTEP diagram of complex **8**. Ellipsoids are drawn at the 50% probability level. Hydrogen atoms are omitted for clarity. Selected distances [Å] and bond angles [°]: Rh1–C1 2.0775(15), Rh1–C8 2.0828(15), Rh1–F1 2.1360(9), Rh1–P3 2.3470(4), Rh1–P1 2.3502(4), Rh1–P2 2.3836 (4), C1–C2 1.539(2), C1–Rh1–F1 173.53(5), C8–Rh1–F1 96.96(5), C1–Rh1–P3 93.56(4), C8–Rh1–P3 87.01(4), F1–Rh1–P3 92.84(3), P3–Rh1–P1 168.314(15), C1–Rh1–P2 90.47(4), C8–Rh1–P2 172.89(4), F1–Rh1–P2 90.08(3), P3–Rh1–P2 93.662(15), P1–Rh1–P2 92.732(16).

with a doublet of quartets (J = 19.9, 6.6 Hz) at 24.0 ppm in the $^{13}C\{^1H\}$ NMR spectrum being assigned as the α carbon atom. In the $^1H\{^{19}F\}$ NMR spectrum the proton resonances are simplified to a triplet of pseudo triplets at 3.15 ppm and a triplet of triplets of doublets at 2.56 ppm. Similar data are obtained for complex **10′** where couplings to the labelled carbon atom are observed with values of 1.9 and 2.1 Hz for the β and α carbon, respectively. These couplings might suggest a *trans* arrangement to the carbonyl ligand which is consistent with the fluorido ligand in the *trans* position to the aromatic ring as described for complex **7**; however a *cis* arrangement cannot be excluded. The signal for the carbonyl ligand of complex **10′** was revealed in the APT NMR spectrum at 189.5 ppm as a doublet of doublet of triplets due to couplings to rhodium, the metal-bound fluorido ligand and the two phosphorus atoms (41.3, 14.8 and 10.9 Hz, respectively). In the ^{19}F NMR spectrum a signal for the rhodium bound fluorido ligand appeared as a broad signal at −425.3 ppm for complex **10**.[63] In the IR spectrum of complex **10** an absorption band at 2056 cm^{-1} can be assigned to the carbonyl ligand which is in agreement with data for other Rh(III) carbonyl complexes.[70,71] The band appears at 2002 cm^{-1} for the isotopologue **10′**, where the isotopic shift is in accordance with literature data.[36]

In contrast to all these observations, treatment of **5** with pentafluorostyrene (ratio 1 : 1.3) at 333 K for 1 d led to a C–F bond activation at the 4-position to yield $[Rh(4\text{-}C_6F_4CHCH_2)(PEt_3)_3]$ (**12**) and the fluorido complex $[Rh(F)(PEt_3)_3]$ (**13**)[60] as well as the hydrogenation product ethylpentafluorobenzene **9**[59] in a ratio of 1.5 : 1.6 : 1 (determined by ^{19}F NMR spectroscopy) (Scheme 4). An independent experiment shows that after an initial formation of **2** at room temperature (see above), the generation of **12** is also observed after heating.

The observed C–F bond activation resembles a reaction pathway, which was previously observed for other substrates.[5,39,58] The generation of a Rh–C bond furnishes initially HF, which in turn can give with complex **5** the rhodium fluorido complex **13** and H_2 or a dihydrido fluorido complex.[60] Subsequently, compound **9** can be generated by a hydrogenation reaction of pentafluorostyrene in the presence of H_2.

In the $^{31}P\{^1H\}$ NMR spectrum of complex **12** a doublet of multiplets was observed at 18.4 ppm with rhodium–phosphorus coupling constant of 138.1 Hz for the phosphine ligand in the *trans* position to the fluorinated moiety. A doublet of doublets at 14.0 ppm showed a rhodium–phosphorus coupling constant of 141.1 Hz and phosphorus–phosphorus coupling constant of 40.1 Hz for the two phosphine ligands in a mutually *trans* arrangement. In the ^1H NMR spectrum, three resonances appeared as a doublet of doublets ($^3J_{(H,H)}$ = 18.1, $^3J_{(H,H)}$ = 12.1 Hz), a doublet ($^3J_{(H,H)}$ = 18.1 Hz) and a doublet ($^3J_{(H,H)}$ = 12.1 Hz) at 6.98, 6.20 and 5.33 ppm, respectively, which are assigned to the olefinic moiety. The coupling of 18.1 Hz confirms the existence of protons in the *trans* position while 12.1 Hz is a typical coupling for protons in the *cis* arrangement.[72–74] Finally, in the ^{19}F NMR spectrum, two signals appeared as multiplets at −110.7 and −147.3 ppm in a ratio of 1 : 1 due to the equivalent fluorine atoms, which confirms that the C–F bond activation takes place at the 4-position of the perfluorinated ring.[8,9,39,43,58]

C–H bond activation reaction

$[Rh(Me)(PEt_3)_3]$ (**14**)[75] is known to be a suitable precursor for C–H bond activation reactions.[5,9,35,39] Therefore, it was also interesting to test its reactivity towards pentafluorostyrene in order to achieve a C–H bond activation instead of the C–F bond activation described above. Indeed, treatment with pentafluorostyrene (ratio 1 : 1.1) in THF at room temperature afforded the C–H bond activation complex $[Rh(E\text{-}CHCHC_6F_5)(PEt_3)_3]$ (**15**) after 30 min as a brown oil (Scheme 5).

After isolation, the $^{31}P\{^1H\}$ NMR spectrum of **15** depicted a doublet of triplets at 19.4 ppm ($^1J_{(Rh,P)}$ = 115.7, $^2J_{(P,P)}$ = 36.1 Hz) and a doublet of doublets at 16.6 ppm ($^1J_{(Rh,P)}$ = 156.7, $^2J_{(P,P)}$ = 36.1 Hz) in a integration ratio of 1 : 2. In the ^1H NMR spectrum, a doublet of multiplets and a doublet of doublet of quadruplets, both as a broad doublets in the phosphorus decoupled NMR spectrum, appeared at 9.18 and 6.42 ppm, respectively. The coupling constant between both resonances of 18.6 Hz indicates an *E*-configuration at the double bond. Based on the data for $[Rh(E\text{-}CHCHCF_3)(PEt_3)_3]$,[35] the signal at lower field can be assigned to the proton at the α-position to

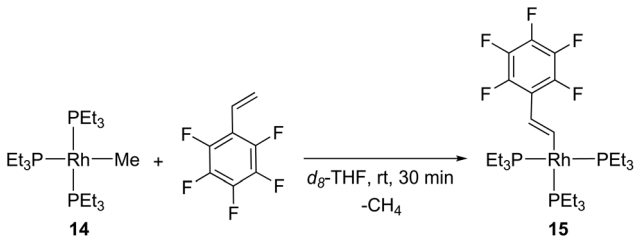

Scheme 5 Reaction of complex **14** with pentafluorostyrene.

Published on 16 Nhlangula 2019. Downloaded by Fail Open on 2025-05-07 08:30:15.

the rhodium nucleus (J = 1.9 Hz), while the β-position proton showed a coupling constant of 6.7 Hz to the *trans* phosphorus ligand. Furthermore, LIFDI MS data revealed a peak with m/z 650 for complex **15**.

Stoichiometric hydroboration reactions

Hydroboration reactions are widely employed to access borylated building blocks.[28,76–84] Thus, [Rh(H)(PEt$_3$)$_3$] (**5**), pentafluorostyrene and HBpin were reacted in a ratio of 1 : 1 : 2.5 in d_8-toluene at room temperature for 5 min to afford the Markovnikov hydroboration compound [C$_6$F$_5$CH(Bpin)CH$_3$] (**16**),[26] small amounts of the anti-Markovnikov product [C$_6$F$_5$CH$_2$CH$_2$(Bpin)] (**17**),[26] the diborylated derivative [C$_6$F$_5$CH$_2$CH(Bpin)$_2$] (**18**)[26] as well as the hydrogenation compound **9** in a ratio of 92 : 2 : 4 : 2. Regarding the rhodium species, the rhodium(III) complex *fac*-[Rh(H)$_2$(Bpin)(PEt$_3$)$_3$] (**19**)[79] was identified as the only product after the catalytic reaction was stopped (Scheme 6). Comparably, treatment of [Rh(Bpin)(PEt$_3$)$_3$] (**1**), pentafluorostyrene and HBpin in a ratio of 1 : 1 : 1.25 in d_{14}-methylcyclohexane at room temperature for 5 min gave the same organic compounds in a ratio of 49 : 14 : 22 : 15 as well as the rhodium(III) complex **19**. It is known that treating complex **5** with HBpin gives complex *fac*-[Rh(H)$_2$(Bpin)(PEt$_3$)$_3$] (**19**),[79] whereas as described above a reaction of **5** with pentafluorostyrene yields **2**. However, in the hydroboration reaction, introducing the reactants in different orders did not lead to different results (Scheme 6).

Two possible pathways can be proposed for the formation of the main hydroboration product, which are depicted in Scheme 7. They are consistent with plausible mechanisms pro-

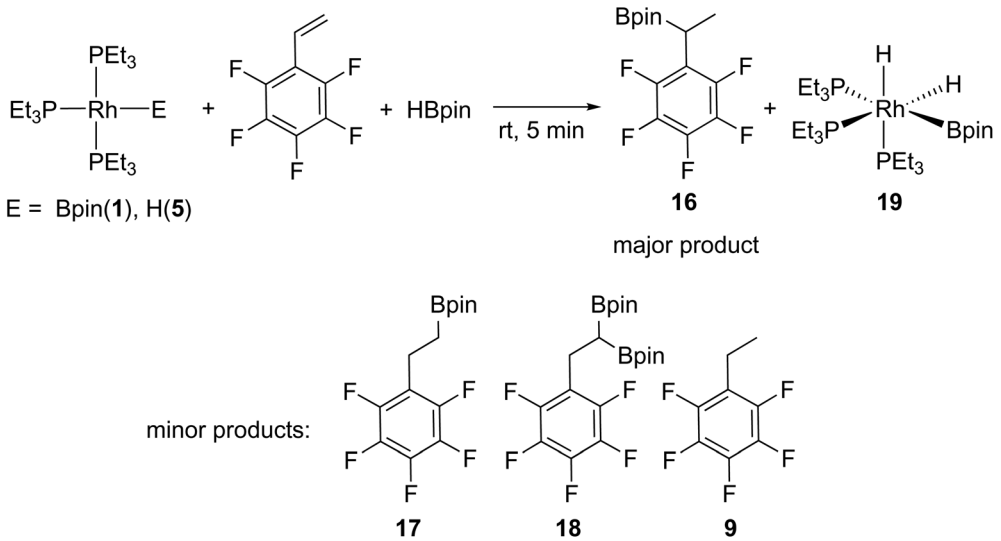

Scheme 6 Stoichiometric hydroboration reactions using complexes **1** or **5**.

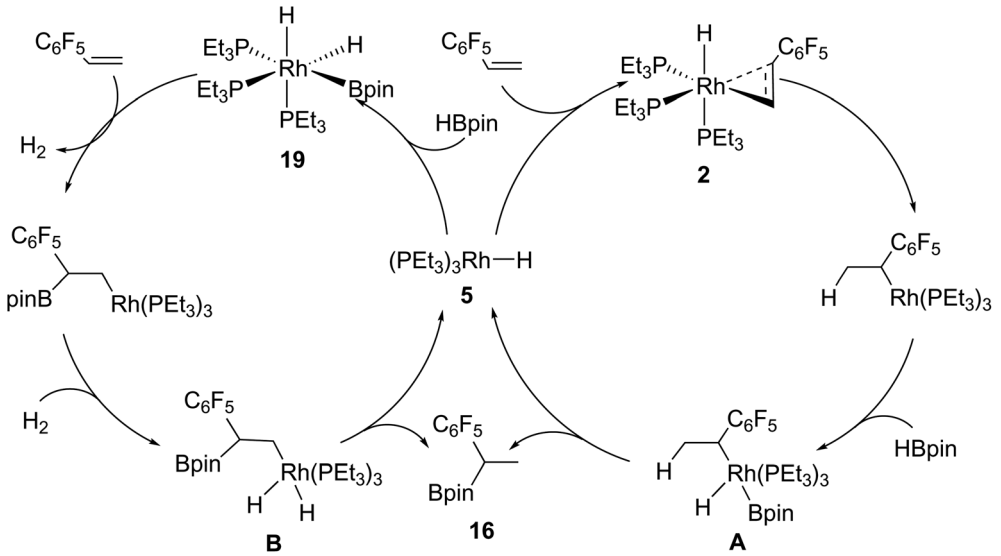

Scheme 7 Possible pathways for the formation of the main hydroboration product.

 This journal is © The Royal Society of Chemistry 2019

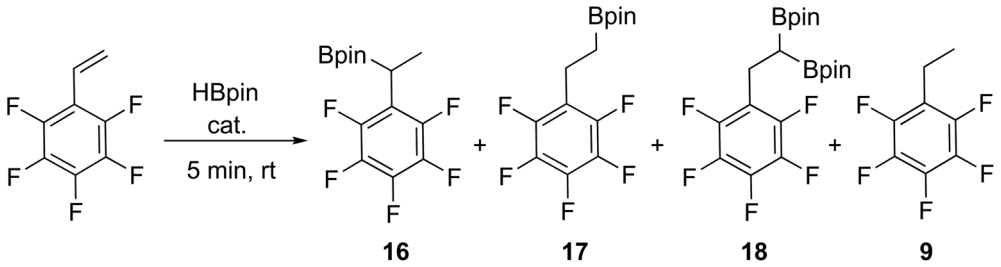

Scheme 8 Catalytic reactions of pentafluorostyrene and HBpin.

Published on 16 Nhlangula 2019. Downloaded by Fail Open on 2025-05-07 08:30:15.

posed for Ti or other Rh complexes.[85–87] Treatment of complex **5** and pentafluorostyrene would yield complex **2**, which after insertion of the olefin into the Rh–H bond and a subsequent oxidative addition of HBpin gives complex **A**. After reductive elimination, the hydroboration product is formed regenerating complex **5**. Alternatively, complex **5** and HBpin afford the oxidative addition complex **19**. Insertion of pentafluorostyrene might occur *via* an initial reductive elimination of H_2 or a dissociation of a phosphine. After oxidative addition of H_2 or rebinding of the phosphine, complex **B** might be generated. Again, the product **16** is formed after a reductive elimination reaction.

Catalytic hydroboration reactions

Considering previous work, in which complexes **1** and **5** were used as catalysts for various reactions such as borylation, C–H and C–F bond activation reactions,[32,36,55,58,79] attention was turned to the catalytic hydroboration reactions (Scheme 8). The reaction of pentafluorostyrene, HBpin (ratio 1 : 1.5) and the rhodium hydrido complex [Rh(H)(PEt_3)$_3$] (**5**) (3 mol% catalyst based on pentafluorostyrene) as the catalyst in C_6D_6 was studied at room temperature. After 5 min, NMR spectroscopic data revealed full conversion of pentafluorostyrene into the same organic products as found in the stoichiometric hydroboration reaction in a ratio of 91 : 6 : 1 : 2 (according to the ^{19}F NMR spectrum) (Table 1 entry 1). The selectivity towards compound **16** decreased to 81% when employing [Rh(Bpin)(PEt_3)$_3$] (**1**) (3.7 mol%) as the catalyst (Table 1 entry 2) and $Me_3SiSiMe_3$ as solvent. Under neat condition, a reaction with complex **5** (1.5 mol%) in pentafluorostyrene also gave full conversion, but less selectively for compound **16** (75%) (Table 1 entry 3).

Table 1 Catalysts comparison of hydroboration reaction of pentafluorostyrene

Catalyst	Solvent	mol%	Conversion[a] (%)	Ratio[b] **16 : 17 : 18 : 9**
5	C_6D_6	3	>99	91 : 6 : 1 : 2
1	$Me_3SiSiMe_3$	3.7	>99	81 : 9 : 3 : 3[c]
5	Neat	1.5	>99	75 : 13 : 4 : 8

[a] Based on pentafluorostyrene consumption. [b] Based on NMR measurements. [c] 4% on an unknown product are present.

Conclusion

In summary, we reported stoichiometric reactions of the rhodium boryl complex [Rh(Bpin)(PEt_3)$_3$] (**1**) and the rhodium hydrido complex [Rh(H)(PEt_3)$_3$] (**5**) towards pentafluorostyrene or its borylated derivative, affording coordination and subsequent C–F bond activation. Aromatic C–F bond activation occurred at the 4-position or 2-position depending on the reaction temperature. The rhodacycle *trans*-[Rh(F)(CH_2CH_2(2-C_6F_4))(PEt_3)$_2$] (**7**) was detected after treatment of **5** with pentafluorostyrene at room temperature. It converted very slowly into [Rh(2-$C_6F_4CHCH_2$)(PEt_3)$_3$] (**6**). A C–H bond activation was achieved when employing the rhodium methyl complex [Rh(Me)(PEt_3)$_3$] (**14**) as the starting material. In stoichiometric and catalytic hydroboration reactions, pentafluorostyrene and HBpin were converted into the Markovnikov addition hydroboration product **16**.

Conflicts of interest

There are no conflicts to declare.

Acknowledgements

We would like to acknowledge Dr Mike Ahrens for fruitful discussions and the China Scholarship Council for financial support.

Notes and references

1 P. Jeschke, *ChemBioChem*, 2004, **5**, 570–589.
2 K. Müller, C. Faeh and F. Diederich, *Science*, 2007, **317**, 1881–1886.
3 Y. Zhou, J. Wang, Z. Gu, S. Wang, W. Zhu, J. L. Aceña, V. A. Soloshonok, K. Izawa and H. Liu, *Chem. Rev.*, 2016, **116**, 422–518.
4 T. Braun and F. Wehmeier, *Eur. J. Inorg. Chem.*, 2011, **2011**, 613–625.
5 T. Ahrens, M. Ahrens, T. Braun, B. Braun and R. Herrmann, *Dalton Trans.*, 2016, **45**, 4716–4728.
6 T. Ahrens, M. Teltewskoi, M. Ahrens, T. Braun and R. Laubenstein, *Dalton Trans.*, 2016, **45**, 17495–17507.

Published on 16 Nhlangula 2019. Downloaded by Fail Open on 2025-05-07 08:30:15.

7 A. L. Raza, M. F. Kuehnel, M. Talavera, M. Teltewskoi, M. Ahrens, P. Kläring, T. Braun and D. Lentz, *J. Fluorine Chem.*, 2018, **214**, 80–85.
8 R. J. Lindup, T. B. Marder, R. N. Perutz and A. C. Whitwood, *Chem. Commun.*, 2007, 3664–3666.
9 A. L. Raza and T. Braun, *Chem. Sci.*, 2015, **6**, 4255–4260.
10 B. Procacci, Y. Jiao, M. E. Evans, W. D. Jones, R. N. Perutz and A. C. Whitwood, *J. Am. Chem. Soc.*, 2015, **137**, 1258–1272.
11 M. Aizenberg and D. Milstein, *Science*, 1994, **265**, 359–361.
12 T. Ahrens, J. Kohlmann, M. Ahrens and T. Braun, *Chem. Rev.*, 2015, **115**, 931–972.
13 T. Braun, F. Wehmeier and K. Altenhöner, *Angew. Chem., Int. Ed.*, 2007, **46**, 5321–5324.
14 L. Zámostná, S. Sander, T. Braun, R. Laubenstein, B. Braun, R. Herrmann and P. Kläring, *Dalton Trans.*, 2015, **44**, 9450–9469.
15 W.-H. Guo, Q.-Q. Min, J.-W. Gu and X. Zhang, *Angew. Chem., Int. Ed.*, 2015, **54**, 9075–9078.
16 J. F. Hartwig, *Chem. Soc. Rev.*, 2011, **40**, 1992–2002.
17 H. Li, K.-H. He, J. Liu, B.-Q. Wang, K.-Q. Zhao, P. Hu and Z.-J. Shi, *Chem. Commun.*, 2012, **48**, 7028–7030.
18 J. P. Collman, Z. Wang, A. Straumanis, M. Quelquejeu and E. Rose, *J. Am. Chem. Soc.*, 1999, **121**, 460–461.
19 A. T. Normand, C. G. Daniliuc, B. Wibbeling, G. Kehr, P. Le Gendre and G. Erker, *J. Am. Chem. Soc.*, 2015, **137**, 10796–10808.
20 X. Xu, G. Kehr, C. G. Daniliuc and G. Erker, *J. Am. Chem. Soc.*, 2015, **137**, 4550–4557.
21 I. Ojima, K. Kato, M. Okabe and T. Fuchikami, *J. Am. Chem. Soc.*, 1987, **109**, 7714–7720.
22 H. C. Brown, G.-M. Chen, M. P. Jennings and P. V. Ramachandran, *Angew. Chem., Int. Ed.*, 1999, **38**, 2052–2054.
23 P. V. Ramachandran, M. P. Jennings and H. C. Brown, *Org. Lett.*, 1999, **1**, 1399–1402.
24 A. M. Segarra, C. Claver and E. Fernandez, *Chem. Commun.*, 2004, 464–465.
25 A. Black, J. M. Brown and C. Pichon, *Chem. Commun.*, 2005, 5284–5286.
26 D. I. McIsaac, S. J. Geier, C. M. Vogels, A. Decken and S. A. Westcott, *Inorg. Chim. Acta*, 2006, **359**, 2771–2779.
27 P. V. Ramachandran and M. P. Jennings, *J. Fluorine Chem.*, 2007, **128**, 827–831.
28 S. Kisan, V. Krishnakumar and C. Gunanathan, *ACS Catal.*, 2017, **7**, 5950–5954.
29 R. Xu, G.-p. Lu and C. Cai, *New J. Chem.*, 2018, **42**, 16456–16459.
30 W. A. Herrmann and S. J. Eder, *Chem. Ber.*, 1993, **126**, 31–37.
31 L. Cronin, C. L. Higgitt, R. Karch and R. N. Perutz, *Organometallics*, 1997, **16**, 4920–4928.
32 M. Teltewskoi, J. A. Panetier, S. A. Macgregor and T. Braun, *Angew. Chem., Int. Ed.*, 2010, **49**, 3947–3951.
33 M. Teltewskoi, S. I. Kalläne, T. Braun and R. Herrmann, *Eur. J. Inorg. Chem.*, 2013, **2013**, 5762–5768.
34 T. Braun, D. Noveski, M. Ahijado and F. Wehmeier, *Dalton Trans.*, 2007, 3820–3825.
35 M. Talavera, C. N. von Hahmann, R. Müller, M. Ahrens, M. Kaupp and T. Braun, *Angew. Chem., Int. Ed.*, 2019, **58**, 10688–10692.
36 C. N. von Hahmann, M. Talavera, C. Xu and T. Braun, *Chem. – Eur. J.*, 2018, **24**, 11131–11138.
37 T. G. Appleton, H. C. Clark and L. E. Manzer, *Coord. Chem. Rev.*, 1973, **10**, 335–422.
38 B. J. Coe and S. J. Glenwright, *Coord. Chem. Rev.*, 2000, **203**, 5–80.
39 A. L. Raza, J. A. Panetier, M. Teltewskoi, S. A. Macgregor and T. Braun, *Organometallics*, 2013, **32**, 3795–3807.
40 J. A. Hatnean, M. Shoshani and S. A. Johnson, *Inorg. Chim. Acta*, 2014, **422**, 86–94.
41 M. W. Drover, L. L. Schafer and J. A. Love, *Dalton Trans.*, 2015, **44**, 19487–19493.
42 T. Piou, F. Romanov-Michailidis, M. Romanova-Michaelides, K. E. Jackson, N. Semakul, T. D. Taggart, B. S. Newell, C. D. Rithner, R. S. Paton and T. Rovis, *J. Am. Chem. Soc.*, 2017, **139**, 1296–1310.
43 S. A. Johnson, E. T. Taylor and S. J. Cruise, *Organometallics*, 2009, **28**, 3842–3855.
44 S. I. Kalläne, T. Braun, B. Braun and S. Mebs, *Dalton Trans.*, 2014, **43**, 6786–6801.
45 L. Keyes and J. A. Love, *C-H and C-X Bond Functionalization: Transition Metal Mediation*, The Royal Society of Chemistry, 2013.
46 E. Clot, O. Eisenstein, N. Jasim, S. A. Macgregor, J. E. McGrady and R. N. Perutz, *Acc. Chem. Res.*, 2011, **44**, 333–348.
47 M. K. Whittlesey and E. Peris, *ACS Catal.*, 2014, **4**, 3152–3159.
48 T. Fujita, K. Fuchibe and J. Ichikawa, *Angew. Chem., Int. Ed.*, 2019, **58**, 390–402.
49 M. F. Kuehnel, D. Lentz and T. Braun, *Angew. Chem., Int. Ed.*, 2013, **52**, 3328–3348.
50 J.-D. Hamel and J.-F. Paquin, *Chem. Commun.*, 2018, **54**, 10224–10239.
51 J. L. Kiplinger, T. G. Richmond and C. E. Osterberg, *Chem. Rev.*, 1994, **94**, 373–431.
52 H. Amii and K. Uneyama, *Chem. Rev.*, 2009, **109**, 2119–2183.
53 H. Torrens, *Coord. Chem. Rev.*, 2005, **249**, 1957–1985.
54 N. A. LaBerge and J. A. Love, in *Organometallic Fluorine Chemistry*, ed. T. Braun and R. Hughes, Springer, Cham, 2015, vol. 52.
55 S. I. Kalläne and T. Braun, *Angew. Chem., Int. Ed.*, 2014, **53**, 9311–9315.
56 T. Beweries, L. Brammer, N. A. Jasim, J. E. McGrady, R. N. Perutz and A. C. Whitwood, *J. Am. Chem. Soc.*, 2011, **133**, 14338–14348.
57 Z. Chen, C.-Y. He, Z. Yin, L. Chen, Y. He and X. Zhang, *Angew. Chem., Int. Ed.*, 2013, **52**, 5813–5817.
58 S. I. Kalläne, M. Teltewskoi, T. Braun and B. Braun, *Organometallics*, 2015, **34**, 1156–1169.

 This journal is © The Royal Society of Chemistry 2019

Published on 16 Nhlangula 2019. Downloaded by Fail Open on 2025-05-07 08:30:15.

59 Y. Sun, H. Sun, J. Jia, A. Du and X. Li, *Organometallics*, 2014, **33**, 1079–1081.
60 T. Braun, D. Noveski, B. Neumann and H.-G. Stammler, *Angew. Chem., Int. Ed.*, 2002, **41**, 2745–2748.
61 G. Meier and T. Braun, *Angew. Chem., Int. Ed.*, 2011, **50**, 3280–3284.
62 H. Baumgarth, G. Meier, T. Braun and B. Braun-Cula, *Eur. J. Inorg. Chem.*, 2016, **2016**, 4565–4572.
63 N. Pfister, T. Braun, P. Wittwer and M. Ahrens, *Z. Anorg. Allg. Chem.*, 2018, **644**, 1064–1070.
64 M. Wozniak, T. Braun, M. Ahrens, B. Braun-Cula, P. Wittwer, R. Herrmann and R. Laubenstein, *Organometallics*, 2018, **37**, 821–828.
65 J. Cámpora, J. A. López, P. Palma, D. del Rio, E. Carmona, P. Valerga, C. Graiff and A. Tiripicchio, *Inorg. Chem.*, 2001, **40**, 4116–4126.
66 J. Cámpora, M. a. del Mar Conejo, K. Mereiter, P. Palma, C. Pérez, M. L. Reyes and C. Ruiz, *J. Organomet. Chem.*, 2003, **683**, 220–239.
67 W. D. Jones, M. G. Partridge and R. N. Perutz, *J. Chem. Soc., Chem. Commun.*, 1991, 264–266.
68 J. K. MacDougall, M. C. Simpson, M. J. Green and D. J. Cole-Hamilton, *J. Chem. Soc., Dalton Trans.*, 1996, 1161–1172.
69 G. Gregorio, G. Pregaglia and R. Ugo, *Inorg. Chim. Acta*, 1969, **3**, 89–93.
70 D. Noveski, T. Braun, B. Neumann, A. Stammler and H.-G. Stammler, *Dalton Trans.*, 2004, 4106–4119.
71 J. Rankin, A. C. Benyei, D. J. Cole-Hamilton and A. D. Poole, *Chem. Commun.*, 1997, 1835–1836.
72 T. Braun, J. Izundu, A. Steffen, B. Neumann and H.-G. Stammler, *Dalton Trans.*, 2006, 5118–5123.
73 X. Zhang, S. Fan, C.-Y. He, X. Wan, Q.-Q. Min, J. Yang and Z.-X. Jiang, *J. Am. Chem. Soc.*, 2010, **132**, 4506–4507.
74 A. Singh, C. J. Fennell and J. D. Weaver, *Chem. Sci.*, 2016, **7**, 6796–6802.
75 P. Zhao and J. F. Hartwig, *Organometallics*, 2008, **27**, 4749–4757.
76 H. C. Brown and B. C. S. Rao, *J. Am. Chem. Soc.*, 1959, **81**, 6428–6434.
77 J. A. Soderquist, J. C. Colberg and L. Del Valle, *J. Am. Chem. Soc.*, 1989, **111**, 4873–4878.
78 J. Schneider, C. P. Sindlinger, S. M. Freitag, H. Schubert and L. Wesemann, *Angew. Chem., Int. Ed.*, 2017, **56**, 333–337.
79 T. Braun, M. Ahijado-Salomon, K. Altenhöner, M. Teltewskoi and S. Hinze, *Angew. Chem., Int. Ed.*, 2009, **48**, 1818–1822.
80 D. Noh, H. Chea, J. Ju and J. Yun, *Angew. Chem., Int. Ed.*, 2009, **48**, 6062–6064.
81 E. E. Touney, R. Van Hoveln, C. T. Buttke, M. D. Freidberg, I. A. Guzei and J. M. Schomaker, *Organometallics*, 2016, **35**, 3436–3439.
82 M. Rauch, S. Ruccolo and G. Parkin, *J. Am. Chem. Soc.*, 2017, **139**, 13264–13267.
83 J. D. Hewes, C. W. Kreimendahl, T. B. Marder and M. F. Hawthorne, *J. Am. Chem. Soc.*, 1984, **106**, 5757–5759.
84 S. A. Westcott, H. P. Blom, T. B. Marder and R. T. Baker, *J. Am. Chem. Soc.*, 1992, **114**, 8863–8869.
85 X. He and J. F. Hartwig, *J. Am. Chem. Soc.*, 1996, **118**, 1696–1702.
86 S. A. Westcott, T. B. Marder and R. T. Baker, *Organometallics*, 1993, **12**, 975–979.
87 K. Burgess, W. A. Van der Donk, S. A. Westcott, T. B. Marder, R. T. Baker and J. C. Calabrese, *J. Am. Chem. Soc.*, 1992, **114**, 9350–9359.